Optical modulator on silicon employing germanium quantum wells

Jonathan E. Roth[1*], Onur Fidaner[1], Rebecca K. Schaevitz[1], Yu-Hsuan Kuo[1,2], Theodore I. Kamins[1,3], James S. Harris, Jr.[1], and David A. B. Miller[1]

[1]*Department of Electrical Engineering, Stanford University, Stanford, CA 94305, USA*
[2]*Department of Electrical Engineering and the Graduate Institute of Electronics Engineering, National Taiwan University, Taipei, Taiwan*
[3]*Quantum Science Research, Hewlett-Packard Laboratories, Palo Alto, CA 94304, USA*
**Corresponding author: jonroth@stanford.edu*

Abstract: We demonstrate an electroabsorption modulator on a silicon substrate based on the quantum confined Stark effect in strained germanium quantum wells with silicon-germanium barriers. The peak contrast ratio is 7.3 dB at 1457 nm for a 10 V swing, and exceeds 3 dB from 1441 nm to 1461 nm. The novel side-entry structure employs an asymmetric Fabry-Perot resonator at oblique incidence. Unlike waveguide modulators, the design is insensitive to positional misalignment, maintaining > 3 dB contrast while translating the incident beam 87 μm and 460 μm in orthogonal directions. Since the optical ports are on the substrate edges, the wafer top and bottom are left free for electrical interconnections and thermal management.

OCIS codes: (160.2100) Electro-optical materials ; (230.2090) Electro-optical devices ; (230.4110) Modulators ; (230.5590) Quantum-well devices ; (230.5750) Resonators ; (250.3140) Integrated optoelectronic circuits.

References and links

1. D. A. B. Miller, "Physical reasons for optical interconnection," Int. J. Optoelectron. **11**, 155-168 (1997).
2. D. A. B. Miller, "Rationale and challenges for optical interconnects to electronic chips," Proc. IEEE **88**, 728-749 (2000).
3. R. Soref and B. Bennett, "Electro optical effects in silicon," IEEE J. Quantum Electron. **23**, 123-129 (1987).
4. D. A. B. Miller, D. S. Chemla, T. C. Damen, A. C. Gossard, W. Wiegmann, T. H. Wood and C. A. Burrus, "Electric field dependence of optical absorption near the bandgap of quantum well structures," Phys. Rev. B **32**, 1043-1060 (1985).
5. R. V. Schmidt and I. P. Kaminow, "Metal-diffused optical waveguides in $LiNbO_3$," Appl. Phys. Lett. **25**, 458-460 (1974).
6. K. W. Goossen, J. A. Walker, L. A. D'Asaro, B. Tseng, R. Leibenguth, D. Kossives, D. D. Bacon, D. Dahringer, L. M. F. Chirovsky, A. L. Lentine, D. A. B. Miller "GaAs MQW Modulators Integrated with Silicon CMOS" IEEE Photon. Technol. Lett. **7**, 360-362, 1995.
7. J. Deboeck and G. Borghs, "III-V on Si: heteroepitaxy versus lift-off techniques," J. Cryst. Growth **127,** 85 -92 (1993).
8. A. S. Liu, R. Jones, L. Liao, D. Samara-Rubio, D. Rubin, O. Cohen, R. Nicolaescu, and M. Paniccia, "A high-speed silicon optical modulator based on a metal-oxide semiconductor capacitor," Nature **427**, 615–-618 (2004).
9. D. Marris-Morini, X. Le Roux, L. Vivien, E. Cassan, D. Pascal, M. Halbwax, S. Maine, S. Laval, J. M. Fedeli, and J. F. Damlencourt, "Optical modulation by carrier depletion in a silicon PIN diode," Opt. Express **14**, 10838-10843 (2006).
10. Q. Xu, B. Schmidt, S. Pradhan, and M. Lipson, "Micrometre-scale silicon electrooptic modulator," Nature **435**, 325-327 (2005).
11. Y. Q. Jiang, W. Jiang, L. L. Gu, X. N. Chen, and R. T. Chen, "80-micron interaction length silicon photonic crystal waveguide modulator," Appl. Phys. Lett. **87**, 221105-1-3 (2005).
12. R. S. Jacobsen, K. N. Andersen, P. I. Borel, J. Page-Pedersen, L. H. Frandsen, O. Hansen, M. Kristensen, A. V. Lavrinenko, G. Moulin, H. Ou, C. Peucheret, B. Zsidri, and A. Bjarklev, "Strained silicon as a new electro-optical material," Nature **441**, 199-202 (2006).
13. P. Yu, J. Wu, and B. Zhu, "Enhanced quantum-confined Pockels effect in SiGe superlattices," Phys. Rev. B **73**, 235328-1-7 (2006).

#81006 - $15.00 USD Received 13 Mar 2007; revised 20 Apr 2007; accepted 25 Apr 2007; published 27 Apr 2007

14. J. Liu, D. Pan, S. Jongthammanurak, K. Wada, L. C. Kimerling, and J. Michel, "Design of monolithically integrated GeSi electro-absorption modulators and photodetectors on an SOI platform," Opt. Express **15**, 623-628 (2007).
15. Y.-H. Kuo, Y. Lee, Y. Ge, S. Ren, J. E. Roth, T. I. Kamins, D. A. B. Miller, and J. S. Harris, "Strong quantum-confined Stark effect in germanium quantum-well structures on silicon," Nature **437**, 1334-1336 (2005).
16. Y.-H. Kuo, Y. K. Lee, Y. Ge, S. Ren, J. E. Roth, T. I. Kamins, D. A. B. Miller, and J. S. Harris Jr., "Quantum-confined stark effect in Ge/SiGe quantum wells on Si for optical modulators," IEEE J. Sel. Top. Quantum Electron. **12**, 1503-1513 (2006).
17. O. Qasaimeh and P. Bhattacharya, "SiGe-Si quantum-well electroabsorption modulators," IEEE Photon. Technol. Lett. **10** 807 – 809 (1998).
18. Y. Miyake, J. Y. Kim, Y. Shiraki, and S. Fukatsu, "Absence of Stark shift in strained $Si_{1-x}Ge_x$/Si type-I quantum wells," Appl. Phys. Lett. **68**, 2097-2099 (1996).
19. M. Whitehead and G. Parry, "High-contrast reflection modulation at normal incidence in asymmetric multiple quantum well Fabry-Perot structure," Electron. Lett. **25**, 566-568 (1989).
20. N. C. Helman, J. E. Roth, D. P. Bour, H. Altug, and D. A. B. Miller, "Misalignment-tolerant surface-normal low-voltage modulator for optical interconnects," IEEE J. Sel. Top. Quantum Electron. **11**, 338-342 (2005).
21. S. B. Samavedam, M. T. Currie, T. A. Langdo, and E. A. Fitzgerald, "High-quality germanium photodiodes integrated on silicon substrates using optimized relaxed graded buffers," Appl. Phys. Lett. **73**, 2125-2127 (1998).
22. H.-C. Luan, D. R. Lim, K. K. Lee, K. M. Chen, J. G. Sandland, K. Wada, and L. C. Kimerling, "High-quality Ge epilayers on Si with low threading-dislocation densities," Appl. Phys. Lett. **75**, 2909-2911 (1999).
23. A. Nayfeh, C. O. Chui, K. C. Saraswat, and T. Yonehara, "Effects of hydrogen annealing on heteroepitaxial-Ge layers on Si: Surface roughness and electrical quality," Appl. Phys. Lett. **85**, 2815-2817(2004).
24. S. Adachi, "Model dielectric constants of Si and Ge," Phys. Rev. B **38**, 12966-12976 (1988).
25. D. J. Godbey, A. H. Krist, K. D. Hobart, and M. E. Twigg, "Selective removal of $Si_{1-x}Ge_x$ from (100) Si using HNO_3 and HF," J. Electrochem. Soc. **139**, 2943-2947 (1992).

1. Introduction

Efficient integration of fast, low-power optical modulators with silicon electronics could benefit telecommunications by reducing cost and improving functionality, and could also make attractive possible low-cost optical interconnects at shorter distances between or even within machines [1, 2]. Until recently, due to a lack of strong electro optic mechanisms in silicon for modulating the refractive index or absorption coefficient [3], most efforts to develop modulators for data transmission were based on materials such as III-V semiconductors employing quantum confined Stark effect (QCSE) electroabsorption [4] and linear electro-optic materials such as lithium niobate [5]. Devices fabricated in these materials require extra processing steps for integration with silicon circuitry, such as flip-chip hybrid integration and epitaxial liftoff [6, 7]. Recently silicon-based modulators have gained much attention, with several devices reported using the free carrier plasma dispersion effect [8,9], including examples employing ring resonators [10] and photonic crystals [11] to increase the interaction of light with the active material. Strained silicon and strained SiGe composites display a linear electro-optic refractive index modulation which has been exploited in several devices [12,13], and an electroabsorption modulator was demonstrated based on the Franz-Keldysh effect in strained SiGe [14].

We recently reported the discovery of a strong QCSE in compressively strained Ge quantum wells (QWs) with SiGe barriers [15, 16], based on the strong direct-gap absorption in Ge near 1500 nm wavelength. This electroabsorption greatly exceeded that of previous attempts based on indirect absorption in SiGe QWs [17, 18]. The large fractional and absolute absorption coefficient contrast and broad bandwidth of absorption modulation demonstrated in our work suggest the possibility of broad-bandwidth, low-insertion-loss modulators without the need for high-Q resonators, long optical path lengths, or even without waveguides and the corresponding precise alignment requirements. This QCSE in Ge has also specifically been demonstrated to operate in the C-band by heating devices to temperatures compatible with CMOS operation [16]. The performance of the Ge QCSE appears to be comparable to or better than the QCSE in III-V devices at similar wavelengths and hence such Ge devices could potentially displace III-V modulators for such wavelengths.

#81006 - $15.00 USD Received 13 Mar 2007; revised 20 Apr 2007; accepted 25 Apr 2007; published 27 Apr 2007

In our previous demonstration of the QCSE, we obtained the absorption coefficient of the structure from photocurrent measurements, not from measured transmission changes. Here we measure the transmitted light to demonstrate the first optoelectronic modulator based on the QCSE from direct-bandgap confinement in group IV materials. A novel asymmetric Fabry-Perot architecture with oblique incidence is employed to maintain an adequate contrast ratio and bandwidth with a reasonable voltage swing while avoiding the tight alignment constraints for coupling to waveguide modulators. The optical input and output ports are on the polished edges of the substrate, freeing the top and bottom for making the many electrical connections required on typical chips and for removing heat. In a first, non-optimized device structure, the modulator displays a peak contrast ratio (CR) of 7.3 dB at 1457 nm wavelength, has a CR greater than 3 dB over a 20 nm range for a voltage swing of 10 V, and an alignment tolerance of 87 μm and 460 μm in orthogonal directions

2. Device concept

The side-entry modulator concept is illustrated in Fig. 1. A converging beam enters the substrate material through a polished edge facet. The beam is focused from the substrate side onto a mesa containing the optically active material. A pair of reflectors within the mesa form a resonant cavity which enhances the interaction of the light with the optically active material. Total reflection at the top reflector can be obtained with total internal reflection (as in our present device) or by another mechanism, and the reflection at the bottom can be achieved with a dielectric interface (as in our present device) or a high-reflectivity dielectric stack. Light reflected from the cavity is coupled out of a substrate edge facet nominally parallel to the entry facet.

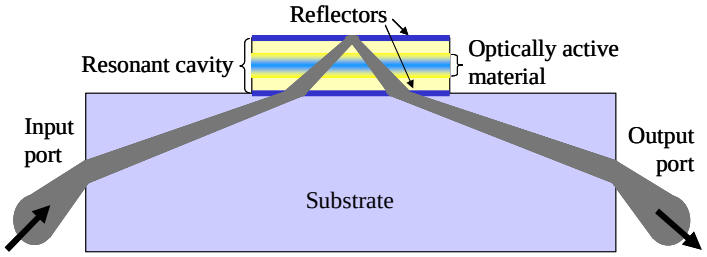

Fig. 1. Side-entry optoelectronic modulator schematic. The thickness of the optically active material is exaggerated here. In the actual device, beams reflecting within the resonant cavity overlap with one another.

Asymmetric Fabry-Perot cavities containing electro absorbing material have been used as reflection modulators, and have the attractive property that their output can be turned nearly completely off when operating on resonance by setting the front and back effective reflectivities equal through absorption modulation [19]. The current work and a previous modulator design [20] employ asymmetric Fabry-Perot modulators with obliquely incident beams. Oblique incidence is advantageous because the interaction length of the beam with the optically active material will be a factor of $1/\cos(\theta)$ longer per pass than in normal incidence, where θ is the angle of the beam relative to normal within the optically active material. Dielectric interfaces and stacks of materials with differing refractive indices are commonly used to make reflectors. At oblique incidence, the reflectivity of such reflectors can be quite high, even for dielectric stack mirrors with small numbers of layers, and especially for TE polarized light which, unlike TM polarized light, does not have a Brewster's angle at which complete transmission occurs.

In our implementation of the side-entry modulator concept, the substrate is Si and the mesa is formed from relaxed bulk $Si_{0.1}Ge_{0.9}$ layers surrounding a nominally strain-balanced superlattice of quantum wells and barriers which display variable electroabsorption with

#81006 - $15.00 USD Received 13 Mar 2007; revised 20 Apr 2007; accepted 25 Apr 2007; published 27 Apr 2007

electric field due to the QCSE. In this material system, it is relatively difficult to create a high-reflectivity dielectric interface or layer stack; the large (4%) lattice mismatch between Si and Ge prevent the growth of thick layers of these materials on one another, especially if crystal quality is to be maintained. Typically, growth of Ge-rich material upon Si relies upon the growth of a graded buffer of several microns thickness [21] or makes use of high-temperature anneal steps to cause relaxation of the Ge-rich buffer and defect density reduction [22, 23]. Anneal steps may lead to a diffused junction of graded composition, which may complicate efforts to create the sharp dielectric boundaries that have high reflectivity.

Though the interdiffusion profile and refractive indices in our sample are not precisely known, the benefits of oblique incidence can be illustrated through a numerical example. At 1455 nm the real components of refractive index of Si and Ge are respectively 3.53 and 4.35 [24], so the index of $Si_{0.1}Ge_{0.9}$ is approximately 4.28 by linear interpolation. The reflectivity of an abrupt Si/$Si_{0.1}Ge_{0.9}$ interface is therefore 0.9% at normal incidence, while for TE polarized light at an angle of incidence of 78.4º from the normal in Si (as occurs in our structure), the reflection coefficient is 31.6%, leading to a stronger cavity resonance. The angle to the normal in $Si_{0.1}Ge_{0.9}$ will be 53.9º, increasing the length of the optical path through the cavity by a factor of 1.7 and consequently increasing absorption per pass.

3. Devices

Epitaxial layers containing 10, 20, 40, and 60 QWs were grown on silicon wafers by reduced pressure chemical vapor deposition. A 1 μm thick boron doped $Si_{0.1}Ge_{0.9}$ buffer was grown in two stages, each followed by high temperature anneals [15, 23]. Next, a thin undoped layer of $Si_{0.1}Ge_{0.9}$ was grown, followed by multiple quantum wells (MQW) in a superlattice of 15.5 nm Ge well layers separated by ~ 33 nm thick $Si_{0.16}Ge_{0.84}$ barriers. Last, a thin undoped $Si_{0.1}Ge_{0.9}$ layer and an n-doped $Si_{0.1}Ge_{0.9}$ layer were grown. Layer thicknesses were determined after growth by secondary ion mass spectrometry (SIMS), scanning electron microscopy, and, for the Ge quantum well widths, quantum mechanical fitting of QCSE transition energies.

Photodiode mesas were lithographically defined on the epitaxial surface, and samples were etched to allow contacting of the p-type layer. Ti/Al ring contacts were evaporated to contact both n- and p-type layers. A mesa fabricated on the 40 QW sample is schematically illustrated in Fig. 2.

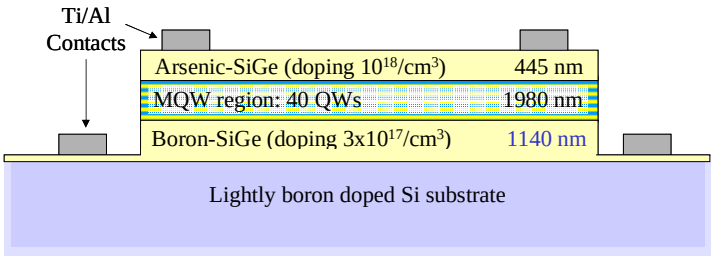

Fig. 2. Diagram of the PIN diode mesa fabricated in a sample with 40 quantum wells for side-entry modulation, not to scale.

#81006 - $15.00 USD Received 13 Mar 2007; revised 20 Apr 2007; accepted 25 Apr 2007; published 27 Apr 2007

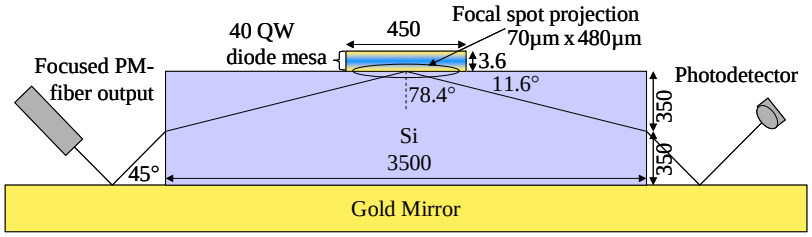

Fig. 3. Diagram of side-entry modulator in experimental setup, not to scale. All unlabelled units are microns.

Modulator chips were cleaved into pieces containing one dimensional arrays of devices, and edges of the chips were polished to form parallel and optically flat facets. The thicknesses of the top $Si_{0.1}Ge_{0.9}$ layers of the devices were individually adjusted using a wet etch that did not attack the polished edges of the silicon substrate [25]. Device arrays were placed on a gold mirror for testing. The testing configuration is shown in Fig. 3. Light from a tunable laser through a polarization-maintaining (PM) fiber is focused towards the mirror at a 45º angle to the surface. Upon reflection, it is coupled through the edge facet of the modulator array substrate. The beam impinges upon the diode mesa from the substrate side at a 78.4º angle from normal incidence. The beam is TE polarized with respect to the Si/SiGe interface, and the beam diameter is at a minimum where it reaches the mesa. The incident Gaussian beam waist diameter is ~ 70 µm, such that the projection of the beam spot on the mesa top surface plane is elliptical with major and minor axes of 480 µm and 70 µm. The mesas are square with 450 µm sides, so there may be a small amount of truncation of the beam by the mesa in one direction. In the mesas, an optical resonator cavity is formed around the MQW region by the total internal reflections at the SiGe/air interface, and Fresnel reflections at the Si/SiGe interface. Light not absorbed in the mesa region is reflected and exits the side of the wafer opposite the side where it entered. The output light bounces off the gold mirror and is collected by an InGaAs photodetector.

Pieces of the wafers were processed separately for electroabsorption measurements of quantum wells. The whole back surfaces were antireflection-coated, as were lithographically defined regions on the front side on top of the mesas. Transmission spectroscopy was performed in which the tunable laser was focused with normal incidence on a device (a "surface-normal" configuration) as the laser wavelength and reverse bias voltage were scanned. Photocurrent in the device mesa was recorded, as was the optical power transmitted through the device. The backsides of these pieces were subsequently coated with aluminum, and the double pass reflectivity was also measured as wavelength and voltage were scanned.

4. Results

The transmission spectra from the antireflection-coated sample with 60 QWs were normalized to transmission through air, and the data are shown in Fig. 4, where the reverse bias voltage was varied from 0.5 V to 18.5 V in 2 V increments. The spectrum from the 60 QW sample very closely matched the cube of the fraction of light transmitted through the 20 QW sample, indicating that the loss on transmission is almost all due to absorption in the quantum wells and not to substrate or other losses. Buffer and substrate thicknesses were about the same in these two wafers, and the magnitude of reflections from the top and bottom of the wafers are expected to be the same for the two samples as well. We matched the measured spectra with results from a simulation of energy level shifts calculated by the tunneling resonance method to determine that the Ge QWs are ~ 15.5 nm wide.

#81006 - $15.00 USD Received 13 Mar 2007; revised 20 Apr 2007; accepted 25 Apr 2007; published 27 Apr 2007

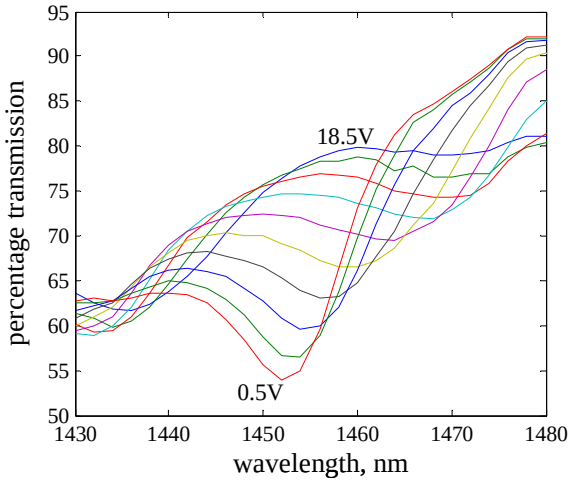

Fig. 4. Transmission of a 60 QW sample for applied reverse biases from 0.5 V to 18.5 V in 2 V increments, measured in the "surface normal" configuration with anti-reflection coatings on both sides.

The intrinsic region in the 60 QW sample is about 3.1 um thick, which is determined from the SIMS measurement of a 10 QW sample, assuming the growth rates were the same in these growths. Thus, for an applied voltage of V_a, the electric field in the quantum well region is approximately (V_a + 0.8)/3.1 V/μm (presuming a built-in voltage ~ 0.8 V). The largest field in the data of Fig. 4 is therefore ~ 11 V/μm (1.1 x 10^5 V/cm). The peak absorption coefficient (averaged through the MQW region) with 0.5 V applied field at the exciton peak closest to the band edge is 2090 cm^{-1} at 1452 nm.

In a double-pass “surface-normal” modulator configuration using this 60 QW sample, with an antireflection-coated top surface and an aluminum-coated bottom surface, the CR was 3.0 dB at 1453 nm for a voltage swing of 18 V, and 2.3 dB for a 10 V swing.

A side-entry modulator with 40 QWs was tested. Light transmitted through the device along the path described in Fig. 3 was measured as the bias voltage and wavelength were scanned. The fraction of light transmitted was calculated by normalizing the data to the intensity of light transmitted through air. The CR for 0 V to 10 V reverse bias is shown in Fig. 5. For a 10 V swing, the peak CR was 7.3 dB at 1457 nm, and the CR was greater than 3 dB from 1461 nm to 1481 nm. Given a total intrinsic region of 2.1μm including doping offset from the MQWs, the electric fields at 0 V and 10 V are approximately 3.8 x 10^3 V/cm and 5.1 x 10^4 V/cm.

A second small local maximum in contrast was observed centered at 1560 nm, showing that the free spectral range of the resonant cavity is about 110 nm, suggesting that the cavity is operating at about 14^{th} order. Given the refractive index and beam angle in the mesa, this suggests the optical cavity length is about 4.0 μm, roughly in agreement with the length calculated from the growth rates.

#81006 - $15.00 USD Received 13 Mar 2007; revised 20 Apr 2007; accepted 25 Apr 2007; published 27 Apr 2007

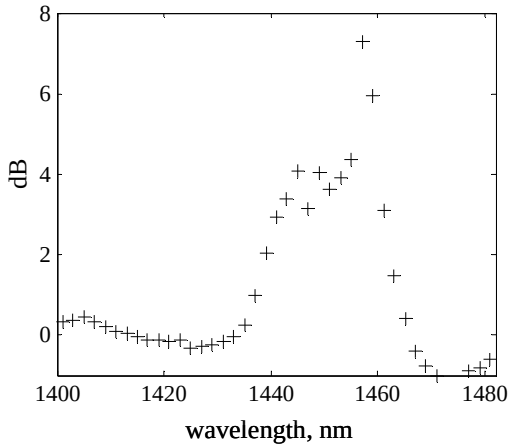

Fig. 5. Contrast ratio from 40 QW sample for 0 V - 10 V reverse bias.

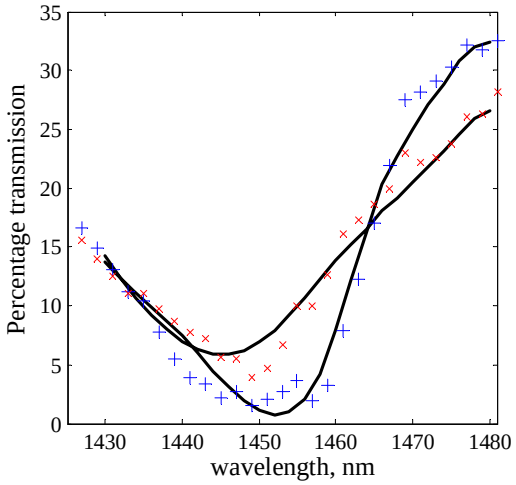

Fig. 6. Percentage of light transmitted through side-entry modulator. Blue "+" points and red "x" points show transmission for 0 V and 10 V reverse bias, respectively, and black lines are simulated transmission. The loss from the two uncoated air/Si interfaces is ~ 68%, indicating that antireflection-coating will greatly increase the transmission.

Reflection from the gold mirrors at 45º incidence was measured to be 99%, and the theoretical fraction of power transmitted at each air/Si boundary (on the sides of the substrate) is 56%, yielding an expected maximum possible transmission through the device of 32%. In the insertion-loss data in Fig. 6, the peak percentage transmission corresponds closely to this loss figure, suggesting that coupling losses could be made very small by antireflection-coating the edge facets. A transfer-matrix calculation of the electromagnetic fields in the epitaxy was used to simulate absorption in the device. The light was treated as a weighted sum of plane waves equivalent to a Gaussian beam with a waist radius of 35 μm. The layer structure simulated consisted of the silicon substrate followed a 120 nm thick layer of refractive index 3.88 to simulate an interdiffused layer between the Si and $Si_{0.1}Ge_{0.9}$, a 1080 nm thick $Si_{0.1}Ge_{0.9}$ layer, a 1980 nm MQW layer, and a top layer of 445 nm of $Si_{0.1}Ge_{0.9}$. The real component of the index of the MQW region was set to 4.28, the same as the $Si_{0.1}Ge_{0.9}$ layers. The addition of the 120 nm layer representing interdiffusion decreases the Si/SiGe interface reflectivity from 32% to 18% in the simulation. The 0 V and 10 V experimental insertion-loss curves for the 40 QW sample were matched to simulations using MQW absorption coefficients taken

#81006 - $15.00 USD Received 13 Mar 2007; revised 20 Apr 2007; accepted 25 Apr 2007; published 27 Apr 2007

from the 2.5 V and 18.5 V transmission curves of the 60 QW sample to get the best fit. These correspond to electric fields of 8.1 x 10^3 V/cm and 5.9 x 10^4 V/cm. The discrepancy in electric fields between the absorption coefficient data and the transmission data it was used to fit are likely due to slight QW thickness variations between wafers. In the simulation, net transmission from mirrors and air/Si interfaces was set to 37% instead of the predicted 31% to better match experimental data. The reflectivity does not quite reach zero in this device, both in simulations and experiments. The finite angular range in the incident beam spot theoretically leads to non-zero reflection in such a device, though we believe here we may just not have quite enough optical absorption to reach the minimum reflectivity possible for this spot size. The minor discrepancies between theory and experiment may be due to the uncertainty in the form of the refractive index grading at the Si to SiGe interface.

The tolerance of the modulator to beam misalignments was tested by setting the wavelength to correspond with the peak CR, and measuring contrast as the laser focusing translation stage was misaligned in the plane of the wafer surface. For translation in the direction parallel to the plane of the edge through which the beam enters the substrate, the CR remained above 3 dB for a 10 V swing over a total translation distance of 460 μm, close to the 450 μm dimension of the device mesa. For translation in the direction normal to the edge where the beam enters, the CR was greater than 3 dB over a total translation distance of 87 μm. For parallel translations, the CR profile was flat-topped, while for normal translation, it was more sharply peaked. In addition to affecting the misalignment tolerance, the choice of mesa size also determines the device capacitance, which was measured to be ~ 10pF. Changing the mesa size should correspondingly change the alignment tolerance, with changes in capacitance in proportion to the changes in device area. Large misalignment tolerance will result in large capacitances that will, however, in practice increase both power dissipation and the difficulty of driving the device at high speed. It may be possible to use smaller spots, for increased alignment tolerance and/or reduced device size and capacitance, though the resonant enhancement in the structure would ultimately be reduced due to the shorter depth of field of the beam.

5. Discussion

The current work demonstrates the viability of the side-entry modulator architecture, as well as the viability of the QCSE in germanium quantum wells for optoelectronic modulation. We should emphasize that the epitaxial structure and mesa size are not optimal, and several improvements in the design are possible. Optimization of the Ge/SiGe quantum well design could lead to greater absorption change in the quantum wells for a given applied electric field. Such optimization could include changing the quantum well thicknesses as well as fabricating them more densely by changing the thickness and composition of strain balanced SiGe barriers. An epitaxy design with optimal layer thicknesses may lead to lower voltage operation, higher CR, and broader optical bandwidth. Calculations suggest that about 68% of the light is lost to reflections at the air/Si interfaces from the beam entering and exiting the substrate. This loss can be minimized through antireflection coating the end facets. Furthermore, operating the devices at temperatures of ~ 90º C, typical in a CMOS chip, will allow for telecommunications C-band operation through shifting the absorption edge to longer wavelengths [16].

The design of the side entry modulators makes them suitable for operation in parallel arrays. As only the edges of the chip are needed for optical interconnection, the top surfaces are left free for electrical interconnection, making the architecture suitable for photonic integrated circuit applications. By relaying the light through the substrate with multiple bounces, optical interconnections could even be made between modulators and detectors on the same chip.

#81006 - $15.00 USD Received 13 Mar 2007; revised 20 Apr 2007; accepted 25 Apr 2007; published 27 Apr 2007

6. Conclusion

In summary, we demonstrate the first optoelectronic modulator employing the quantum confined Stark effect in germanium quantum wells, and also feature a novel side-entry modulator architecture. Devices are fabricated on silicon substrates, making them amenable to integration with silicon electronics. We demonstrate a peak contrast ratio of 7.3 dB for a voltage swing of 10 V at 1457 nm, and the contrast is > 3 dB over a 20 nm range in wavelength. The novel side-entry architecture employs an asymmetric Fabry-Perot cavity at grazing incidence, and avoids the tight alignment constraints and potentially the coupling loss of waveguides, permitting translation of the beam by 87 μm in one direction and 460 μm in the orthogonal direction while maintaining a contrast ratio > 3 dB. As the polished edges of the substrate serve as the optical input and output ports, the top and bottom of the chip are left free for electrical interconnections and thermal management.

Acknowledgments

This work is supported by Intel Corporation, the DARPA/ARO EPIC program, and the MARCO/DARPA FCRP Interconnect Focus Center. The authors wish to thank T. Carver, T. Brand, and R. Macdonald for assistance in fabricating devices, and W. Frans and Lawrence Semiconductor Research Laboratory for epitaxial growth.

#81006 - $15.00 USD Received 13 Mar 2007; revised 20 Apr 2007; accepted 25 Apr 2007; published 27 Apr 2007